UNIVERSITY *of* York

This is a repository copy of *Underwater localization based on grid computation and its application to transmit beamforming in multiuser UWA communications*.

White Rose Research Online URL for this paper:
http://eprints.whiterose.ac.uk/127319/

Version: Accepted Version

Article:

Liao, Li, Zakharov, Yuriy orcid.org/0000-0002-2193-4334 and Mitchell, Paul Daniel orcid.org/0000-0003-0714-2581 (2018) Underwater localization based on grid computation and its application to transmit beamforming in multiuser UWA communications. IEEE Access. pp. 4297-4307. ISSN 2169-3536

eprints@whiterose.ac.uk
https://eprints.whiterose.ac.uk/

Underwater Localization Based on Grid Computation and its Application to Transmit Beamforming in Multiuser UWA Communications

Li Liao[†], *Student Member, IEEE*, Yuriy Zakharov[†], *Senior Member, IEEE*,
Paul D. Mitchell[†], *Senior Member, IEEE*

Abstract—Underwater localization is a challenging problem and established technologies for terrestrial systems cannot be used, notably the Global Positioning System (GPS). In this paper, we propose an underwater localization technique and demonstrate how it can be effectively used for transmit beamforming in multiuser underwater acoustic (UWA) communications. The localization is based on pre-computation of acoustic channel parameters between a transmitter-receiver pair on a grid of points covering the area of interest. This is similar to the localization process using matched field processing, which is often based on processing *a priori* unknown signals received by an array of hydrophones. However, in our case, every receiver is assumed to have a single hydrophone, while an array of transducers transmit (pilot) signals known at a receiver. The receiver processes the received pilot signal to estimate the Channel State Information (CSI) and compares it with the CSI pre-computed on the grid; the best match indicates the location estimate. The proposed localization technique also enables an efficient solution to the inherent problem of informing a transmitter about the CSI available at the receiver for the purpose of transmit beamforming. The receiver only needs to send a grid point index to enable the transmitter to obtain the pre-computed CSI corresponding to the particular grid point, thereby significantly reducing transmission overheads. We apply this approach to a multiuser communication scenario with orthogonal frequency-division multiplexing (OFDM) and show that the proposed approach results in accurate localization of receivers and multiuser communications with a high detection performance.

Keywords—Localization, multiuser communication, SDMA, transmit beamforming

I. INTRODUCTION

In recent years, there has been a growing interest in underwater acoustic communications (UAC) in various application areas such as telemetry, remote control, speech/image transmission, etc. [1]. The investigation of UAC has met many challenges since, in particular, the underwater acoustic (UWA) channels are characterized by limited bandwidth, long propagation delays, and multipath interference [2]. The classical multiple access communication strategies, such as time division multiple access (TDMA), frequency division multiple access (FDMA), code division multiple access (CDMA), as well as spatial division multiple access (SDMA) have been widely used in terrestrial radio communication systems,

with users separated in time, frequency, code domains, or in space [3]–[7]. FDMA is not well suited for UAC due to the narrow bandwidth of the UAW channel. TDMA can be useful, but it is challenging to make efficient use of channel time in highly dynamic scenarios, since long propagation delays inhibit the ability to allocate capacity in response to time varying needs. CDMA may suffer from the severe multipath interference that leads to degradation of the code correlation properties, resulting in smaller codeword distances [5]. These three multiple access schemes have to divide the available time-frequency resources among the multiple users. On the other hand, with SDMA, the same time-frequency resources can be independently used by every user. With simultaneous transmission to multiple users in multi-antenna broadcast channels, SDMA is capable of achieving a much higher throughput than other multiple-access schemes [6], and it is a viable choice in UAC.

In this paper, we consider SDMA systems with multiple transmit antennas (transducers) and multiple receivers equipped with a single antenna (hydrophone) each. In such a system, in order to design the transmit beamformer, the transmitter requires knowledge of the Channel State Information (CSI) between every transducer and every receiver hydrophone [8]. This information can be estimated at the receiver by processing pilot signals. The estimated CSI then needs to be sent back to the transmitter, which can be problematic in narrowband UWA channels due to the large amount of data comprising the CSI and low data throughput capability.

This problem can be resolved if both the transmitter and receiver have a pre-computed dictionary of possible CSIs. In this case, the receiver only needs to send back the index of the CSI from the dictionary that provides the best match to the CSI estimate. In UWA channels, such a dictionary can be built based upon acoustic field computation for a specific environment, where the communication system is installed. More specifically, the dictionary can be computed for a grid of points in space (grid of range/depth points), thus also solving the localization problem (estimation of position of the receiver with respect to the position of the transducers), which is required in many applications [9]–[11]. Underwater localization is a difficult problem, and in many cases it cannot rely on traditional terrestrial localisation technologies, such as the Global Positioning System (GPS) [2].

The approach based on pre-computing the acoustic field using a wave equation is similar to localization using *matched*
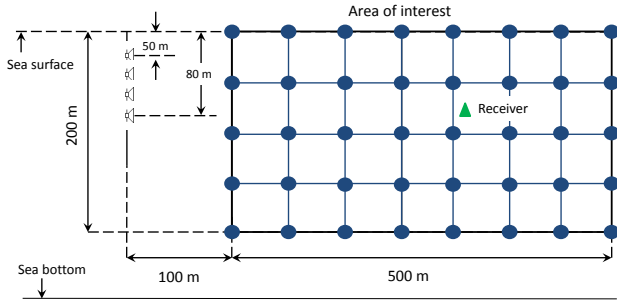
Fig. 1: The receiver is located in an area of interest 200 m × 500 m. The sea depth is 220 m. The transducers are equally spaced from a depth of 50 m to 80 m.

field processing (MFP) often based on processing of *a priori* unknown signals received by an array of hydrophones. There have been a number of studies and experiments related to MFP [12]–[16] and the general idea is to search over a parameter space for the unknown parameters of the signal source [17], [18]. As a development of MFP, the environmental focalization technique was proposed [19], [20], which is based on adjustment of environmental parameters within a search space which, after being optimized under a particular objective function, generates physical parameters that correspond to the acoustic field replica best matching the observed acoustic field. In the recent work [21], the focalization technique was used to improve the channel estimation in UAC.

The design of a transmit beamformer in multiuser channels is an important problem in modern wireless communication systems with SDMA. The main difficulty in such systems is that coordinated receive processing is not possible and that all the signal processing must be employed at the transmitter side [8]. Linear precoding schemes provide a promising trade-off between performance and complexity [22]–[25]. The zero-forcing (ZF) beamforming is the most common linear precoding scheme, which decouples the multiuser channel into multiple independent subchannels [26]–[32]. Orthogonal frequency-division multiplexing (OFDM) communication is considered as a promising technology for high data-rate communications in UAC [33]–[36]. It can be efficiently combined with SDMA to improve the system throughput [33], [37]–[39]. In this paper, we will be investigating transmit beamforming based on linear precoding in an OFDM communication system.

One of the significant problems with numerical investigation of signal processing algorithms in UWA systems is the modeling of the signal transmission that takes into consideration the specific acoustic environment, and consequently the specific multipath propagation. For such virtual signal transmission, i.e., transmission that mimics a real sea trial, the *VirTEX* simulator was developed [40] and used [41]; the model relies on the *Bellhop* ray/beam tracing approach [42] to compute the channel response in defined acoustic environments. A similar approach is used in the *Waymark* simulator [43]–[46] developed to investigate UWA signal transmission in long communication sessions. We use the Waymark model to investigate the localization and communication techniques.

In this paper:

- a receiver localization technique is proposed, based on matching the CSI estimated at the receiver to the CSI pre-computed at grid points in an area of interest (over depth and range);
- we propose to apply this localization technique in UAC with SDMA to inform the transmitter of the CSI when designing the transmit beamformer, thus greatly reducing the size of the feedback message from the receiver to the transmitter;
- a transmit beamformer is proposed, that exploits multiple channel estimates for the same user to improve the detection performance;
- the accuracy of the proposed localization technique and the detection performance of multiuser UAC with OFDM signals and proposed transmit beamforming are investigated using the virtual signal transmission.

This paper is organized as follows. Section II describes the proposed localization technique. Section III describes the proposed transmit beamformer based on the localization technique. Section IV presents numerical results demonstrating that the proposed localization technique is effective in terms of accuracy of localization and that the proposed transmit beamformer achieves a high detection performance. Section V gives some concluding remarks.

II. RECEIVER LOCALIZATION

Consider a (geographical) area of interest, for example as shown in Fig. 1. The Channel State Information (CSI) between a transducer and a receiver hydrophone located within this area can be pre-computed, e.g., using standard acoustic field computation programs. This computation can be repeated for every grid point as illustrated in Fig. 1, thus producing a grid map. The receiver can estimate the CSI using a pilot signal transmitted from the transducer. By comparing the estimated CSI with the CSI in the grid map, the best match can be identified and the position of the corresponding grid point can be treated as an estimate of the receiver position.

Let $\mathbf{g}_m$ be a $K \times 1$ channel frequency response vector representing the CSI for the mth grid point; the vector length K is the number of (subcarrier) frequencies at which the frequency response is defined. UAC typically operates at relatively high frequencies, for which ray tracing is an efficient method to solve the wave equation and thus compute the vector $\mathbf{g}_m$. For our numerical examples, we use the ray-tracing program Bellhop [42]. Based on the knowledge of the acoustic environment, such as the sound-speed profile (SSP) and acoustic parameters of the sea bottom, the depth of the transducer, and the (range-depth) position of the grid point, the program computes the complex-valued amplitudes $A_{m,i}$ and delays $\tau_{m,i}$ for multiple (L_m) rays (eigenpaths), $i = 0, \ldots, L_m - 1$, connecting the transducer and hydrophone at the mth grid point. Based on these channel parameters, the channel frequency response can be computed as

$$g_m(f) = \sum_{i=0}^{L_m-1} A_{m,i}\exp(-j2\pi f\tau_{m,i}), \qquad (1)$$

where the computations are made at subcarrier frequencies $f = f_0, ..., f_{K-1}$ covering the frequency range of the communication system; the values $g_m(f)$ are elements of the vector $\mathbf{g}_m = [g_m(f_0), ..., g_m(f_{K-1})]^T$.

Let $\hat{\mathbf{h}}$ be a $K \times 1$ vector representing the channel estimate at the same frequencies. In the frequency domain, at a frequency f, the received signal is given by

$$y(f) = h(f)p(f) + n(f), \tag{2}$$

where $h(f)$, $p(f)$ and $n(f)$ are the channel frequency response, transmitted signal and noise, respectively. The least-square channel estimate is then given by [47]:

$$\hat{h}(f) = \frac{y(f)}{p(f)}, \quad f = f_0, ..., f_{K-1}. \tag{3}$$

Thus, elements of the $K \times 1$ vector $\hat{\mathbf{h}}$ are the values $\hat{h}(f_k)$, $k = 1, ..., K$, i.e. $\hat{\mathbf{h}} = [\hat{h}(f_0), ..., \hat{h}(f_{K-1})]^T$.

The vector $\mathbf{g}_m$ represents a 'signature' of the mth grid point, and $\hat{\mathbf{h}}$ is a 'signature' measured at the receiver. By comparing $\hat{\mathbf{h}}$ with the M signatures in the dictionary $\{\mathbf{g}_m\}_{m=1}^M$, we can find the best match resulting in an estimate of the receiver location.

We could find the best match between the vector $\hat{\mathbf{h}}$ and M vectors $\{\mathbf{g}_m\}_{m=1}^M$ representing the grid map by computing the normalised covariance

$$c_m = \frac{\left| \mathbf{g}_m^H \hat{\mathbf{h}} \right|^2}{||\mathbf{g}_m||_2^2 \, ||\hat{\mathbf{h}}||_2^2}, \quad m = 1, ..., M, \tag{4}$$

where $||\hat{\mathbf{h}}||_2^2 = \hat{\mathbf{h}}^H \hat{\mathbf{h}}$, and finding the maximum amongst all the covariances:

$$m_{\text{best}} = \arg \max_{m=1,...,M} c_m. \tag{5}$$

However, since the pilot transmission and reception are not synchronized, there is an unknown delay between the channel impulse responses estimated at the receiver and those pre-computed using the wave equation. In application to the channel frequency responses, this is equivalent to replacing $\hat{\mathbf{h}}$ with $\boldsymbol{\Lambda}_\tau \hat{\mathbf{h}}$, where $\boldsymbol{\Lambda}_\tau$ is an $K \times K$ diagonal matrix with diagonal elements

$$\boldsymbol{\Lambda}_\tau = \text{diag} \left[e^{-j2\pi f_0 \tau}, ..., e^{-j2\pi f_{K-1} \tau} \right],$$

and τ is the unknown propagation delay. Therefore, the covariance computed according (4) cannot be directly used to identify the best match. This can be modified by searching for the maximum over a delay range as given by

$$m_{\text{best}} = \arg \max_{m=1,...,M} \frac{\max_{\tau \in [\tau_{\min}, \tau_{\max}]} \left| \mathbf{g}_m^H \boldsymbol{\Lambda}_\tau \hat{\mathbf{h}} \right|^2}{||\mathbf{g}_m||_2^2 \, ||\hat{\mathbf{h}}||_2^2}, \tag{6}$$

where we use the fact that $||\boldsymbol{\Lambda}_\tau \hat{\mathbf{h}}||_2^2 = ||\hat{\mathbf{h}}||_2^2$, and $[\tau_{\min}, \tau_{\max}]$ is an interval of possible delays. Note that the quantities $\mathbf{g}_m^H \boldsymbol{\Lambda}_\tau \hat{\mathbf{h}}$ in (6) can be efficiently computed for a range of delays using the fast Fourier transform (FFT).

With multiple transducers, the localization performance can be improved by combining the coherence coefficients for all (N_T) transducers. More specifically, N_T grid maps $\{\mathbf{g}_{t,m}\}_{m=1}^M$, $t = 1, ..., N_T$, are pre-computed, one for every transducer, N_T channel estimates $\hat{\mathbf{h}}_t$, $t = 1, ..., N_T$, are obtained at the receiver, one for each transducer, and the grid point with the best match is found as

$$m_{\text{best}} = \arg \max_{m=1,...,M} \sum_{t=1}^{N_T} \frac{\max_{\tau \in [\tau_{\min}, \tau_{\max}]} \left| \mathbf{g}_{t,m}^H \boldsymbol{\Lambda}_\tau \hat{\mathbf{h}}_t \right|^2}{||\mathbf{g}_{t,m}||_2^2 \, ||\hat{\mathbf{h}}_t||_2^2}. \tag{7}$$

Geographical coordinates of the grid point m_{best} are considered as an estimate of the receiver location. The accuracy of this localization method is investigated in Section IV.

In the following section, Section III, we show how this localization technique can be used for transmit beamforming in a multiuser communication system.

III. TRANSMIT BEAMFORMING

We consider a scenario with a transmitter using multiple transmit antennas and multiple receivers using single receive antennas. The transmission technique is OFDM with a transmitted signal described by a set of subcarriers at frequencies $f \in \{f_0, ..., f_{K-1}\}$. A broadcast channel with N_R users can be described in the frequency domain as

$$y_n(f) = \mathbf{h}_n^T(f)\mathbf{x}(f) + n_n(f), \quad n = 1, ..., N_R, \tag{8}$$

where $y_n(f)$ is the signal received by the nth receiver at subcarrier f, $\mathbf{h}_n(f) = [h_{n,1}(f), ..., h_{n,N_T}(f)]^T$ is the frequency response of the channel between the transmit antennas and nth receiver at frequency f, $\mathbf{x}(f)$ is the $N_T \times 1$ transmitted signal vector and $n_n(f)$ is Gaussian noise with zero mean and variance $\sigma_n^2(f)$. We also introduce the $N_R \times N_T$ channel matrix $\mathbf{H}(f) = [\mathbf{h}_1(f), ..., \mathbf{h}_{N_R}(f)]^T$. Then the model in (8) can be rewritten as

$$\mathbf{y}(f) = \mathbf{H}(f)\mathbf{x}(f) + \mathbf{n}(f), \tag{9}$$

where $\mathbf{y}(f) = [y_1(f), ..., y_{N_R}(f)]^T$ are signals received by the N_R receivers and $\mathbf{n}(f) = [n_1(f), ..., n_{N_R}(f)]^T$ is the noise vector.

In linear precoding (transmit beamforming) methods, the transmitted signal vector $\mathbf{x}(f)$ is a linear transformation of the information symbols $\mathbf{s}(f) = [s_1(f), ..., s_{N_R}(f)]$ [32]:

$$\mathbf{x}(f) = \mathbf{T}(f)\mathbf{s}(f), \quad f = f_0, ..., f_{K-1}, \tag{10}$$

where $\mathbf{T}(f)$ is an $N_T \times N_R$ precoding matrix (beamformer).

To design $\mathbf{T}(f)$ achieving zero interference between users, the product $\mathbf{H}(f)\mathbf{T}(f)$ should be a diagonal matrix [32] of size $N_R \times N_R$, e.g., the identity matrix $\mathbf{I}_{N_R}$:

$$\mathbf{H}(f)\mathbf{T}(f) = \mathbf{I}_{N_R}. \tag{11}$$

Such a precoder is known as the zero-forcing (ZF) beamformer and it is given by

$$\mathbf{T}(f) = \mathbf{H}^H(f) \left[\mathbf{H}(f)\mathbf{H}^H(f) \right]^{-1}. \tag{12}$$

The detection performance of the receivers can be improved using the diagonal loading:

$$\mathbf{T}(f) = \mathbf{H}^H(f) \left[\mathbf{H}(f)\mathbf{H}^H(f) + \alpha\mathbf{I}_{N_R} \right]^{-1}, \tag{13}$$

where $\alpha > 0$ is associated with different beamforming designs [48]–[50]; for the design of ZF beamforming, $\alpha = 0$. When designing the beamformer, the true channel parameters are unavailable and therefore their estimates are used instead.

Every column $\mathbf{T}^{(n)}(f)$ of the matrix $\mathbf{T}(f)$ is an $N_T \times 1$ beamformer vector dedicated to a single receiver. The transmitted OFDM signal for the nth user after beamforming is given by

$$\mathbf{x}_n(f) = \mathbf{T}^{(n)}(f)s_n(f), \quad f = f_0, ... f_{K-1}, \quad (14)$$

where $s_n(f)$ is the information symbol for the nth user at subcarrier f.

The design of the transmit beamformer requires the channel frequency response from each transmit antenna to be known by the transmitter. A classical method to obtain this knowledge is to send back the estimated channel frequency response from each receiver to the transmitter. Such feedback represents a significant overhead, however, and can comprise a substantial portion of the overall capacity for data throughput. With the proposed localization technique using the grid map, the only information that needs to be sent back to the transmitter is the index number of the grid point where the receiver is located.

To obtain more accurate localization and better detection performance, the resolution of the grid map can be improved; the influence of the map resolution on the localization and detection performance is investigated in Section IV.

Another approach is based on increasing the number of grid points transmission to which is cancelled by the beamformer, as proposed below. With our localization technique, based on grid computation, the full set of position estimates is finite. Therefore, we can find, instead of one location estimate, several estimates, e.g., by finding several (two or three, as in our numerical investigation) grid points with the highest covariances. In this case, the feedback message should contain indices of these grid points. When designing the transmit beamformer, the additional channel estimates can be used to improve the detection performance by cancelling interference in the extra grid points.

To explain the proposed approach in detail, consider an example with $N_T = 4$ transmit antennas and $N_R = 2$ users. When only one location estimate for each user is received at the transmitter in the feedback message, the 2×4 channel matrix is given by $\mathbf{H}(f) = [\mathbf{h}_1(f), \mathbf{h}_2(f)]^T$ and the 4×2 matrix $\mathbf{T}(f)$ is found from (13). Here, the vectors $\mathbf{h}_1(f)$ and $\mathbf{h}_2(f)$ are the frequency responses for the best grid points of user 1 and user 2, respectively, as found by using (7).

With two location estimates for each user, the beamformer vectors for user 1 and user 2 are found by solving, respectively, the following equations:

$$\mathbf{H}_1(f)\mathbf{T}^{(1)}(f) = [1, 0, 0]^T, \quad (15)$$
$$\mathbf{H}_2(f)\mathbf{T}^{(2)}(f) = [0, 0, 1]^T, \quad (16)$$

where $\mathbf{H}_1(f) = [\mathbf{h}_{1,1}(f), \mathbf{h}_{2,1}(f), \mathbf{h}_{2,2}(f)]^T$, $\mathbf{H}_2(f) = [\mathbf{h}_{1,1}(f), \mathbf{h}_{1,2}(f), \mathbf{h}_{2,1}(f)]^T$, and $\mathbf{h}_{p,q}$ is the channel response vector corresponding to the qth location estimate of the pth user. The beamformer found by solving the equation (15) will be focusing the beam towards the best location estimate of

user 1, while focusing zeros to the two location estimates for user 2. The beamformer found by solving the equation (16) will be focusing the beam towards the best location estimate of user 2, while focusing zeros to the two location estimates for user 1. This can significantly reduce the multiuser interference in the case of the best location estimates to be incorrect.

With three location estimates for each user, the beamformer vectors for user 1 and user 2 are found by solving, respectively, the following equations:

$$\mathbf{H}_1(f)\mathbf{T}^{(1)}(f) = [1, 0, 0, 0]^T, \quad (17)$$
$$\mathbf{H}_2(f)\mathbf{T}^{(2)}(f) = [0, 0, 0, 1]^T, \quad (18)$$

where $\mathbf{H}_1(f) = [\mathbf{h}_{1,1}(f), \mathbf{h}_{2,1}(f), \mathbf{h}_{2,2}(f), \mathbf{h}_{2,3}(f)]^T$ and $\mathbf{H}_2(f) = [\mathbf{h}_{1,1}(f), \mathbf{h}_{1,2}(f), \mathbf{h}_{1,3}(f), \mathbf{h}_{2,1}(f)]^T$. In the case of two and three location estimates, the beamforming vectors are found as

$$\mathbf{T}^{(1)}(f) = \left[\mathbf{H}_1^H(f)[\mathbf{H}_1(f)\mathbf{H}_1^H(f) + \alpha\mathbf{I}_{N_R}]^{-1}\right]^{(1)}, (19)$$
$$\mathbf{T}^{(2)}(f) = \left[\mathbf{H}_2^H(f)[\mathbf{H}_2(f)\mathbf{H}_2^H(f) + \alpha\mathbf{I}_{N_R}]^{-1}\right]^{(2)}. (20)$$

With the location of the receiver estimated using the proposed grid map technique, there is no need to have a long feedback message sent back to the transmitter to design the beamformer. Assuming that the total number of grid points in the area of interest (see Fig. 1) is $201 \times 501 < 2^{17}$ (with the 1 m resolution grid map), only 17 bits are required to represent the receiver position on the grid. For two users, the feedback messages contain 34 bits. This is significantly less compared to the case when the CSI estimate is transmitted. Indeed, to transmit frequency responses for $K = 1024$ subcarriers, $N_T = 4$ transducers and $N_R = 2$ users, and with 16 bits representing a complex-valued sample of frequency response, a feedback message comprising $16KN_TN_R = 16 \times 1024 \times 4 \times 2 = 2^{17}$ bits is required. This requires UAC with a very high throughput, and such transmission would be impractical. The proposed approach allows the feedback messages to be reduced in size by $2^{17}/34 \approx 4000$ times. For the grid map with a 0.5-meter resolution, 38 bits (only slightly higher than 34 bits in the case of 1-m resolution) are required for the feedback messages. Thus, UAC with the proposed transmit beamforming allows significant reduction of the feedback messages.

IV. NUMERICAL RESULTS

In this section, numerical examples are presented to illustrate the performance of the proposed receiver localization and transmit beamforming techniques. In the investigation, we use the Waymark simulator [43]–[46] for the virtual signal transmission in scenarios with N_T transducers are investigated. The sea depth is 220 m, and the transducers are equally spaced from a depth of 50 m to 80 m (for $N_T = 4$) or to 100 m (for $N_T = 6$). The transducers emit acoustic signals in the interval of vertical angles $[-50°, +50°]$. The area of interest is shown in Fig. 1. The SSP and sea bottom parameters are taken from [51] and shown in Fig. 2. Every receiver is equipped with a single receive antenna. The signals are transmitted at the carrier frequency 3072 Hz with a frequency bandwidth of 1024 Hz, so that the frequency band is from
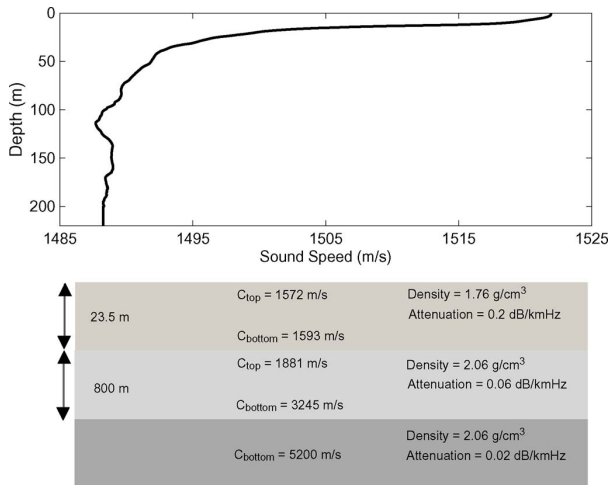
Fig. 2: The SSP and the layered sea bottom parameters.

(a) $d = 50$ m, $r = 200$ m.

(b) $d = 50$ m, $r = 500$ m.

(c) $d = 150$ m, $r = 200$ m.
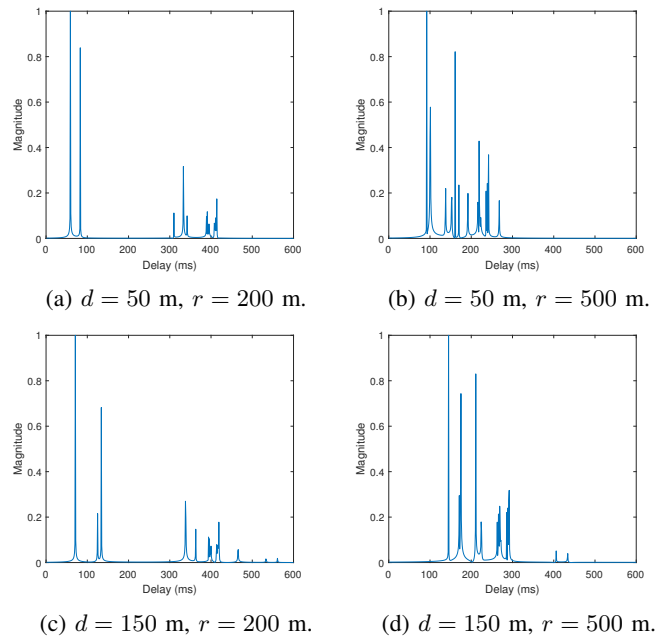
(d) $d = 150$ m, $r = 500$ m.

Fig. 3: Examples of the channel impulse response magnitude for a receiver within the area of interest and for the transducer depth 80 m. The receiver is positioned at a depth d and range r from the transducer.

2560 Hz to 3584 Hz. The pilot and data transmission are performed using OFDM signals with $K = 1024$ subcarriers, an orthogonality interval of 1 s, and subcarrier spacing of 1 Hz. The cyclic prefix (CP) of the OFDM symbols is 1 s long to avoid the intersymbol interference due to long channel delays (see Fig. 3). When searching over delays τ in (7), the search interval $[\tau_{\min}, \tau_{\max}]$ is set to OFDM orthogonality interval $[-0.5, 0.5]$ s. The pilot and data symbols used for modulation of OFDM subcarriers are BPSK symbols.

In the experiments, a grid map, with 1 m or 0.5 m resolution, is generated and stored in memory for every transducer. The grid maps are pre-computed in Matlab (version R2013a) under the Windows 7 operating system with a 3.4 GHz Intel Core i7 CPU and 8 GB of RAM. The 1 m resolution grid map with $201 \times 501 \approx 10^5$ grid points is computed within 5 min, and it requires a storage memory of 37 MB. The 0.5 m resolution grid map with about 4×10^5 grid points is computed within 20 min, and it requires a storage memory of 148 MB. The average computation time and storage memory for one grid point is approximately 3 ms and 370 bytes, respectively.

A. Localization Experiments

To investigate the performance of the localization technique, a pilot signal is transmitted from each of the four transmit antennas sequentially in time. The pilot signal is a single OFDM symbol with a predefined BPSK sequence modulating the subcarriers. At the receiver, channel estimation is carried out as described by (3). Using the channel estimates, the best combined coherence of the channel frequency responses estimated at the receiver and those computed at the grid points is calculated using equation (7). The position of this best grid point is treated as an estimate of the receiver position. The grid map is computed with a resolution of either 1 m or 0.5 m in both the depth and range.

To illustrate the acoustic field in the area of interest, Fig. 4 shows results of the ray tracing in this area. Fig. 3 shows examples of the channel impulse response for four grid points within this area. It is seen that most of the acoustic rays
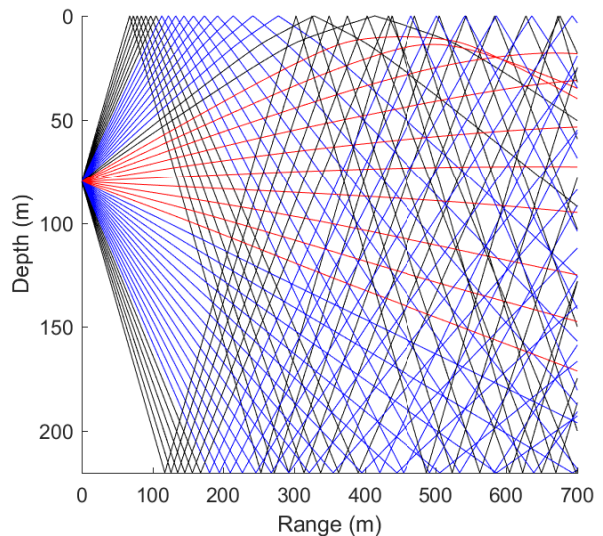

Fig. 4: Ray tracing computation for the area of interest. The rays are plotted using different colors to simply improve the visualization.

experience reflections from the sea surface or bottom. As a result (as can be seen in Fig. 3), the multipath delay spreads can be as high as 0.5 s.

To investigate the probability of correct localization, the localization is performed for 100 different positions of the receiver within the area of interest. The tested positions uniformly cover the area. We consider two cases. In the first case, the received signal is not distorted by the additive noise, i.e., the signal-to-noise ratio is SNR = ∞ dB. In the second case,
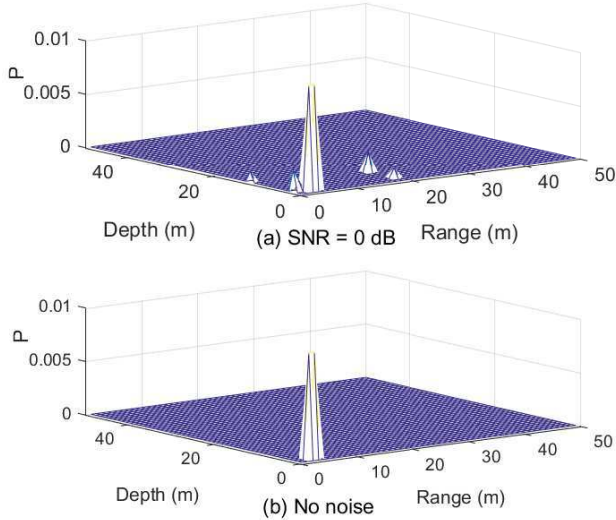
Fig. 5: Distribution of localization errors in the scenario with the flat sea surface. The grid map resolution is 1 m.
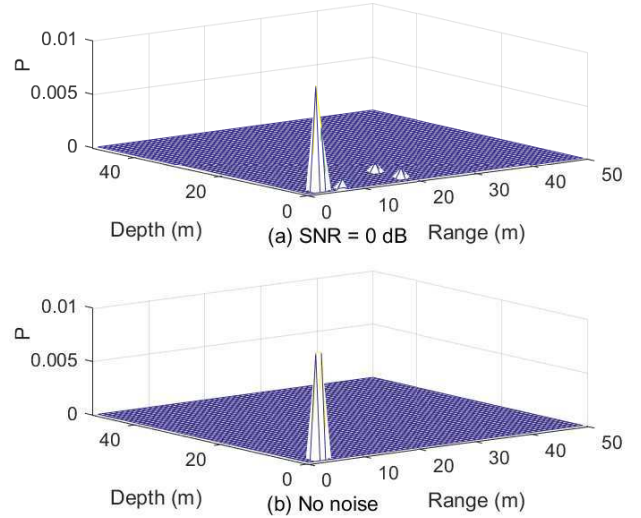

Fig. 6: Distribution of localization errors in the scenario with transmission of pilot signals in an environment where the surface is a sine wave, while the grid map is computed for the flat sea surface. The grid map resolution is 1 m.

white Gaussian noise of the same power as the signal power in the frequency bandwidth of the communication system is added to the received pilot signal, so that SNR = 0 dB; we repeat the experiment 10 times, every time adding a new noise realization, and averaging simulation results over the 10 trials.

Experiments are done in the scenarios as follows.

1) Flat sea surface: The sea surface is flat. The receiver is located exactly on a grid point; more specifically, the set of the receiver depths is given by the vector [11 32 53 74 95 116 137 158 179 199] m and the set of ranges from the transducers is given by the vector [100 150 200 250 300 350 400 450 500 550] m. In both cases (low and high SNR) around 91% of estimates are equal to the true location. Fig. 5 shows the probability of incorrect localization P as function of the difference (in range and depth) between the estimated location and the true location. It can be seen that the incorrect location estimates are mostly close (within a few meters) to the true location.

2) Sinusoidal sea surface: In UWA channels, propagated signals interact with the sea surface. As can be seen in Fig. 4, in the area of interest, many multipath arrivals are reflected from the sea surface, i.e., the sea surface plays an important role in the propagation. Therefore, another test is carried out where the pilot signals are transmitted in the environment with a 'frozen' sinusoidal sea surface, while the channels at grid points are pre-calculated in the environment with a flat calm surface. The amplitude and the wavelength of the sea surface waves are set to be 5 m and 8 m, respectively. The other conditions of the experiment are the same as in the previous scenario. As in the experiment with the flat sea surface, in this experiment for both cases (low and high SNR) around 91% of estimates are equal to the true location. Fig. 6 shows the probability of incorrect estimates against distances to the true location. It can be seen that the location accuracy is high and similar to that in the experiment with the flat sea surface, despite the mismatch of the grid map computation to the true

acoustic environment where the pilot signals propagate.

3) Receivers are located between grid points: To investigate the localization technique in a more practical scenario, an experiment is carried out with the receiver located between grid points; the receiver locations in the experiment with the flat sea surface are now shifted randomly with a uniform distribution within the grid resolution interval. Fig. 7 shows the probability of incorrect localization P as function of the difference between the estimated location and the true location. In this case, over 70% of location estimates still have a distance to the true location less than 5 m, which can be acceptable for some applications. However, it is clear that compared to the two previous scenarios with the receiver at a grid point, the error probability increases. For some receiver positions, the location estimate can differ significantly (of the order of tens of metres) from the true location, even without the noise.

To achieve better localization, we can improve the resolution of the grid map and/or increase the number of transmit antennas. Fig. 8 shows the cumulative distribution function (CDF) of distance between the estimated and true positions for the four combinations of the resolution and number of transmit antennas. An increase in the number of transducers from $N_T = 4$ to $N_T = 6$ greatly improves the localization performance. However, an equivalent effect is achieved with the same number of transmit antennas and an improved resolution of the grid map. The latter can be a more practical approach since it does not require additional hardware at the transmitter.

In Section III, it was proposed to use several location estimates (several estimated grid points) when designing the transmit beamformer. We now investigate the CDF (see Fig. 9) of the distance between the best of two (or three) location estimates and the true location for $N_T = 4$. It is seen that it
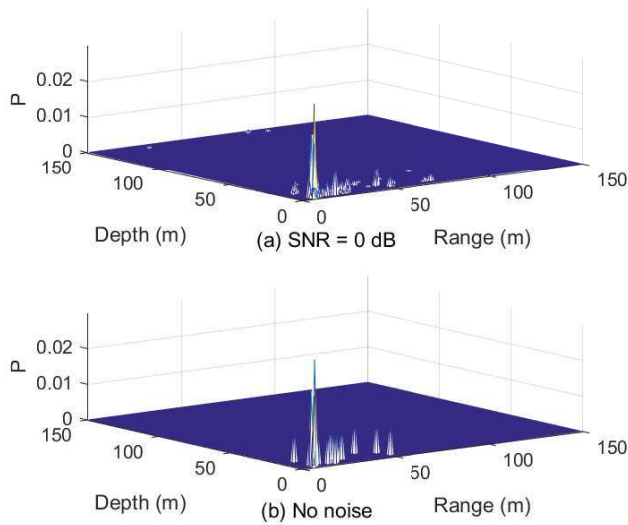
Fig. 7: Distribution of localization errors in the scenario with the receiver at random positions between grid points. The grid map resolution is 1 m.
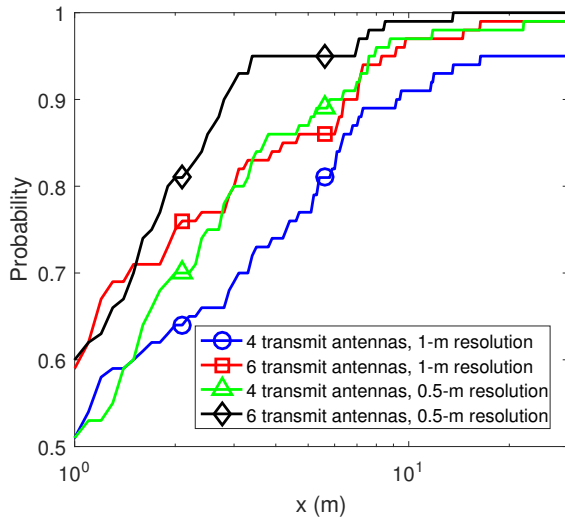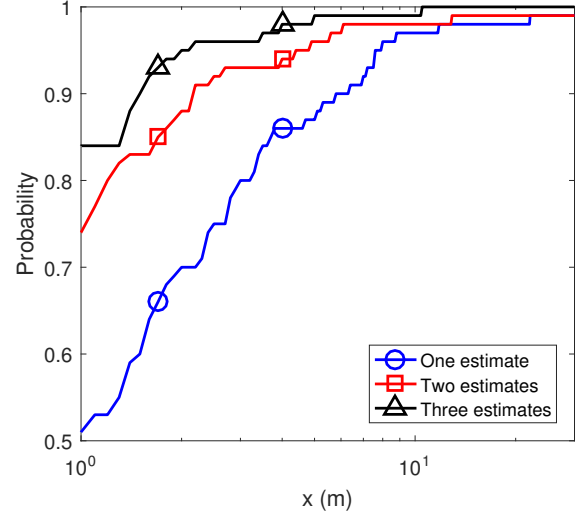

Fig. 9: CDF for the position error x (meters) for the best location estimate of one, two, or three estimates. The grid map is calculated with a resolution of 0.5 m. $N_T = 4$.

Fig. 8: CDF for the position error x (meters), calculated as $x = \sqrt{\Delta_d^2 + \Delta_r^2}$, where Δ_d is the depth error and Δ_r is the range error, for experiments with different grid map resolution and different numbers of transmit antennas.

is highly probable (about 80%) that the best of two and best of three position estimates is within 1 m to the true location, while with a single estimate, the probability is only about 50%.

Numerical results considered in this subsection demonstrate that the proposed localization technique is capable of achieving highly accurate position estimates.

B. Transmit Beamforming Experiments

In this subsection, we consider scenarios with $N_T = 4$ transmit antennas and $N_R = 2$ users (receivers). An experiment contains two stages. At the first stage, the transmitter transmits one pilot OFDM symbol from each transmit antenna,

and the receivers process the received pilot signals as described in subsection IV-A to identify the receiver positions on the grid map. These positions (grid point indices) are sent back to the transmitter, which recovers the CSI of the receivers from the grid map and designs the beamformer $\mathbf{T}$ as explained in Section III.

At the second stage, the transmitter generates $N_T = 4$ signals for transmission by the four transmit antennas from two data packets, represented by vectors $\mathbf{d}_1$ and $\mathbf{d}_2$ in Fig. 10, and intended for the two users. Every 512 bits of each information data packet are encoded into a 1024-bit message using a rate 1/2 convolutional encoder with a generator polynomial matrix [23 35] in octal. The message bits are interleaved and transformed into $K = 1024$ BPSK symbols, corresponding to 1024 subcarriers of a single OFDM symbol for a single user, $s_1(f_k)$ and $s_2(f_k)$, respectively. The BPSK symbols intended for simultaneous transmission to the two users are applied to two jointly developed beamformers, $\mathbf{T}^{(1)}(f_k)$ and $\mathbf{T}^{(2)}(f_k)$. The beamformer outputs are combined at corresponding sub-carriers and corresponding transmit antennas and transformed into the time domain using the inverse FFTs (IFFTs).

A data packet comprising 65536 data bits generates 128 consecutive OFDM symbols as shown in Fig. 11. The 128-length sequence of the information OFDM symbols is appended with 8 pilot OFDM symbols as shown in Fig. 11. In the pilot OFDM symbols, all $K = 1024$ subcarriers are allocated for pilot symbols. At the receiver, eight channel estimates obtained from the eight pilot OFDM symbols are averaged to reduce the noise level in the final estimates. These channel estimates are used for minimum mean-squared error (MMSE) equalization of the information OFDM symbols in the frequency domain and further decoding by the soft-input Viterbi decoder [52].

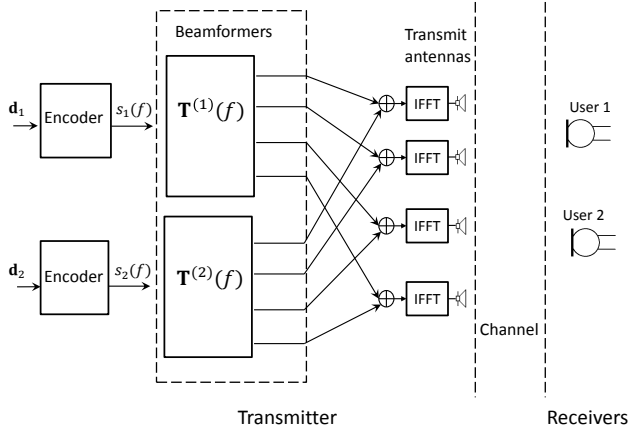Experiments are carried out for the following scenarios.

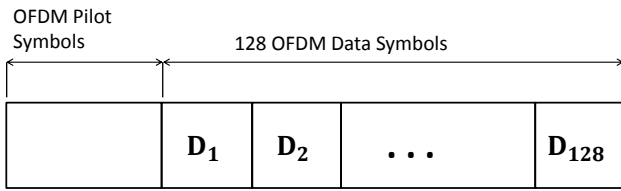Fig. 10: The diagram of the transmit beamforming experiment with four transmit antennas and two users.

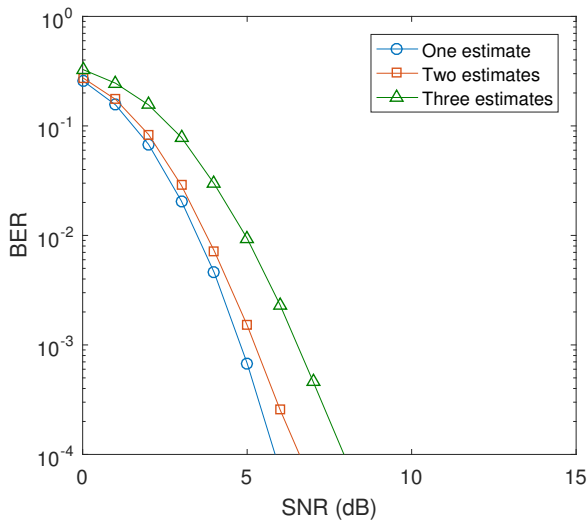Fig. 11: The diagram of the OFDM signal.

Fig. 12: BER performance in Scenario 1. Both the receivers are located at grid points with perfect localization provided by the first estimates.
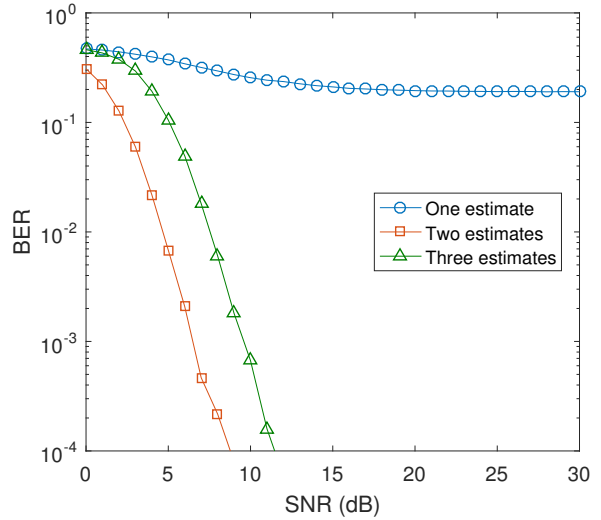

Fig. 13: BER performance in Scenario 2. Both the receivers are located at grid points with perfect localization provided by the second estimates.

1) Scenario 1: In this scenario, both the receivers are located at grid points with perfect localization provided by the first estimates. User 1 is located at a depth of 74 m and range of 200 m from the transmitter, user 2 is located at a depth of 95 m and range 200 m from the transmitter. The BER performance for user 1 is shown in Fig. 12. In this scenario, the best BER performance is achieved by the beamformer designed using the first location estimate for each user, since the first estimates provide true locations of the receivers. Indeed, the BER performance degrades with more location estimates used for the design of the beamformer.

2) Scenario 2: In this scenario, both the receivers are located at grid points with perfect localization provided by the second estimate. User 1 is at a depth of 116 m and range of 200 m from the transmitter, while user 2 is at a depth of 74 m and range of 250 m. The BER performance for user 1 is shown in Fig. 13. The BER performance for the beamformer designed with the first location estimate is poor since the first estimates are not accurate. The beamformer designed with the first and second position estimates has significantly better detection performance. This is because the second estimates are correct in this scenario. When using three position estimates the performance degrades but not significantly.

3) Scenario 3: A more practical situation is considered in this scenario, where the receivers are located between grid points. User 1 is located at a depth of 116.2m and range of 200.4 m from the transmitter, while user 2 is located at a depth of 74.1 m and range of 250.3 m. Both the users are located between grid points, and therefore, all estimated grid points have displacements to the true user positions.

The difference between an estimate and true position results in time shifts (phase distortions) and amplitude differences in the channel frequency responses used for designing the transmit beamformer. Fig. 14 shows the BER performance for this scenario. It can be seen that the beamformers designed using
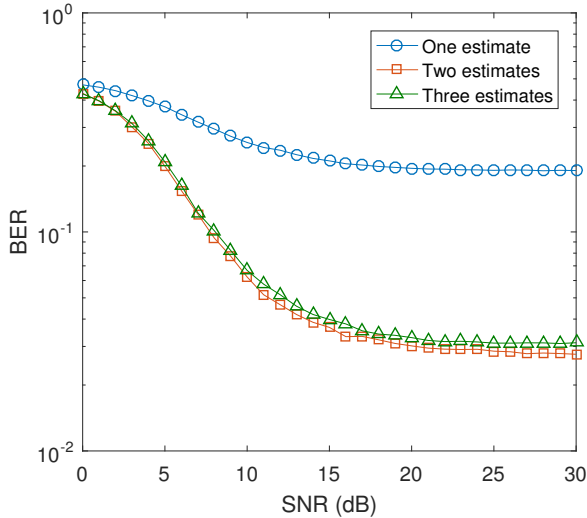
Fig. 14: BER performance of beamformers designed in Scenario 3. The receivers are located between grid points. The grid map resolution is 1 m.
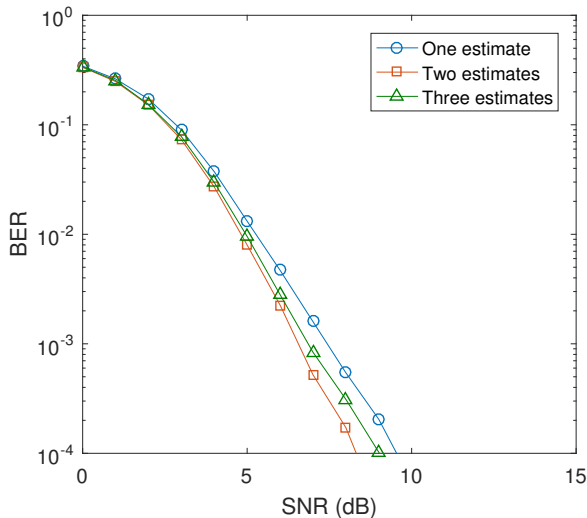

Fig. 15: BER performance of beamformers designed in Scenario 3. The receivers are located between grid points. The grid map resolution is 0.5 m.

the 1-m resolution grid map cannot provide high detection performance, since the position errors are high. To reduce the position errors, a simple idea is to improve the resolution of the grid map. Fig. 15 shows the BER performance for the 0.5 m resolution grid map. It can be seen that in this case, the performance significantly improves.

4) Scenario 4: In this scenario, the propagation channel described by the SSP shown in Fig. 16 is used for signal transmission in the Waymark model. It differs from the assumed channel described by the SSP shown in Fig. 2 which is still used for computation of the grid map. The other simulation parameters are the same as in Scenario 3. It can be seen that the two SSPs significantly differ close to the sea surface. Fig. 17
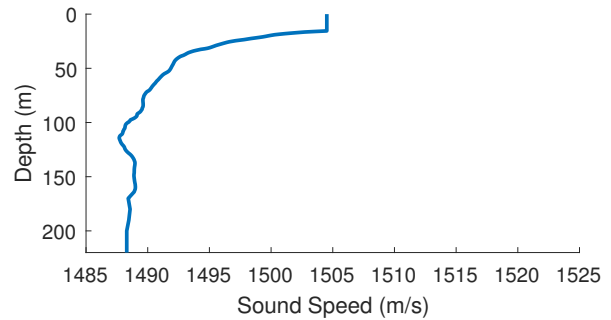

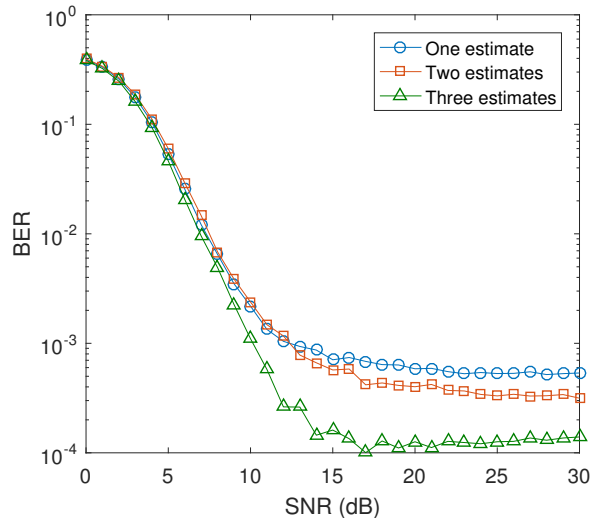Fig. 16: The SSP used for signal transmission in Scenario 4.

Fig. 17: BER performance of beamformers designed in Scenario 4. The receivers are located between grid points. The grid map resolution is 0.5 m. The real SSP (shown in Fig. 16) is different from the SSP used for the grid map computation. Code rate 1/2.

shows the BER performance for the case of the code rate 1/2, the same as used in Scenario 3. By comparing results in Fig. 17 and Fig. 15, one can see that the detection performance of the receiver degrades; more specifically, there is now a floor level due to the multiuser interference that is not cancelled by the beamformer, which is now designed based on the mismatched CSI. However, the receiver can still operate with a BER as low as BER = 10^{-3} . With some sacrifice in the system throughput in this scenario, the detection performance can be significantly improved by using a code rate of 1/3, as illustrated in Fig. 18. Results in Fig. 17 and Fig. 18 also show that the proposed beamformer with multiple channel estimates provides better performance than the single-estimate beamformer.

V. CONCLUSIONS

In this paper, a localization technique has been proposed, which is based on pre-computation of a grid map with CSI defined by the acoustic environment. This technique has been applied to multiuser underwater acoustic communications with multiple transmit antennas; more specifically, the localization
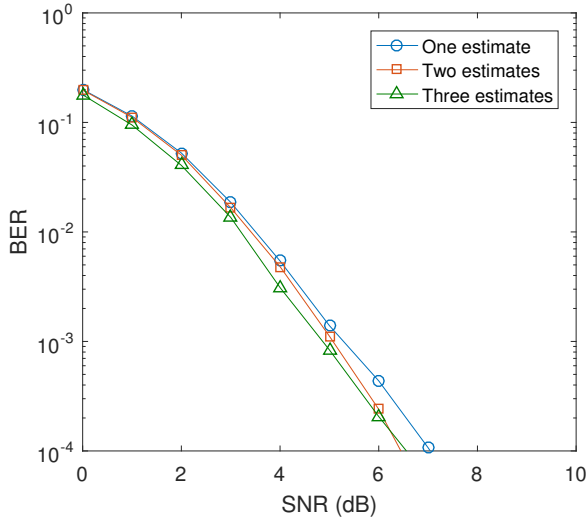
Fig. 18: BER performance of beamformers designed in Scenario 4. The receivers are located between grid points. The grid map resolution is 0.5 m. The real SSP (shown in Fig. 16) is different from the SSP used for the grid map computation. Code rate 1/3.

method has been used for designing the transmit beamforming. We have also proposed a transmit beamforming technique that incorporates multiple location estimates (multiple points on the grid map) for improving the detection performance. Numerical investigation has shown that the proposed techniques allow accurate localization and high detection performance. Importantly, this has been achieved with significant reduction in the size of feedback messages required for designing the beamformer.

REFERENCES

[1] M. Stojanovic, J. Catipovic, and J. G. Proakis, "Adaptive multichannel combining and equalization for underwater acoustic communications," *The Journal of the Acoustical Society of America*, vol. 94, no. 3, pp. 1621–1631, 1993.

[2] W. S. Burdic, *Underwater acoustic system analysis*. Prentice Hall, 1991.

[3] A. Baggeroer, "Acoustic telemetry - An overview," *IEEE Journal of Oceanic Engineering*, vol. 9, no. 4, pp. 229–235, 1984.

[4] J. A. Catipovic, "Performance limitations in underwater acoustic telemetry," *IEEE Journal of Oceanic Engineering*, vol. 15, no. 3, pp. 205–216, 1990.

[5] D. B. Kilfoyle and A. B. Baggeroer, "The state of the art in underwater acoustic telemetry," *IEEE Journal of Oceanic Engineering*, vol. 25, no. 1, pp. 4–27, 2000.

[6] P. Viswanath and D. N. C. Tse, "Sum capacity of the vector Gaussian broadcast channel and uplink-downlink duality," *IEEE Transactions on Information Theory*, vol. 49, no. 8, pp. 1912–1921, 2003.

[7] J.-H. Cui, J. Kong, M. Gerla, and S. Zhou, "The challenges of building mobile underwater wireless networks for aquatic applications," *IEEE Network*, vol. 20, no. 3, pp. 12–18, 2006.

[8] G. Caire and S. Shamai, "On the achievable throughput of a multiantenna Gaussian broadcast channel," *IEEE Transactions on Information Theory*, vol. 49, no. 7, pp. 1691–1706, 2003.

[9] W. Xu, A. B. Baggeroer, and H. Schmidt, "Performance analysis for matched-field source localization: Simulations and experimental results," *IEEE Journal of Oceanic Engineering*, vol. 31, no. 2, pp. 325–344, 2006.

[10] J. Tabrikian and H. Messer, "Three-dimensional source localization in a waveguide," *IEEE Transactions on Signal Processing*, vol. 44, no. 1, pp. 1–13, 1996.

[11] G. Mao, B. Fidan, and B. D. Anderson, "Wireless sensor network localization techniques," *Computer Networks*, vol. 51, no. 10, pp. 2529–2553, 2007.

[12] C. Clay, "Optimum time domain signal transmission and source location in a waveguide," *The Journal of the Acoustical Society of America*, vol. 81, no. 3, pp. 660–664, 1987.

[13] M. J. Hinich, "Maximum-likelihood signal processing for a vertical array," *The Journal of the Acoustical Society of America*, vol. 54, no. 2, pp. 499–503, 1973.

[14] G. C. Carter, "Variance bounds for passively locating an acoustic source with a symmetric line array," *The Journal of the Acoustical Society of America*, vol. 62, no. 4, pp. 922–926, 1977.

[15] H. P. Bucker, "Use of calculated sound fields and matched-field detection to locate sound sources in shallow water," *The Journal of the Acoustical Society of America*, vol. 59, no. 2, pp. 368–373, 1976.

[16] C. Soares, S. M. Jesus, and E. Coelho, "Environmental inversion using high-resolution matched-field processing," *The Journal of the Acoustical Society of America*, vol. 122, no. 6, pp. 3391–3404, 2007.

[17] A. Tolstoy, *Matched field processing for underwater acoustics*. World Scientific, 1993.

[18] A. B. Baggeroer, W. A. Kuperman, and P. N. Mikhalevsky, "An overview of matched field methods in ocean acoustics," *IEEE Journal of Oceanic Engineering*, vol. 18, no. 4, pp. 401–424, 1993.

[19] M. D. Collins and W. Kuperman, "Focalization: Environmental focusing and source localization," *The Journal of the Acoustical Society of America*, vol. 90, no. 3, pp. 1410–1422, 1991.

[20] C. Soares, M. Siderius, and S. M. Jesus, "Source localization in a time-varying ocean waveguide," *The Journal of the Acoustical Society of America*, vol. 112, no. 5, pp. 1879–1889, 2002.

[21] L. P. Maia, A. Silva, and S. M. Jesus, "Environmental model-based time-reversal underwater communications," *IEEE Access, Early Access*, 2017.

[22] A. Wiesel, Y. C. Eldar, and S. Shamai, "Linear precoding via conic optimization for fixed MIMO receivers," *IEEE Transactions on Signal Processing*, vol. 54, no. 1, pp. 161–176, 2006.

[23] M. Stojnic, H. Vikalo, and B. Hassibi, "Rate maximization in multi-antenna broadcast channels with linear preprocessing," *IEEE Transactions on Wireless Communications*, vol. 5, no. 9, pp. 2338–2342, 2006.

[24] M. Joham, W. Utschick, and J. A. Nossek, "Linear transmit processing in MIMO communications systems," *IEEE Transactions on Signal Processing*, vol. 53, no. 8, pp. 2700–2712, 2005.

[25] S. Shi, M. Schubert, and H. Boche, "Downlink MMSE transceiver optimization for multiuser MIMO systems: Duality and sum-MSE minimization," *IEEE Transactions on Signal Processing*, vol. 55, no. 11, pp. 5436–5446, 2007.

[26] Q. H. Spencer, A. L. Swindlehurst, and M. Haardt, "Zero-forcing methods for downlink spatial multiplexing in multiuser MIMO channels," *IEEE Transactions on Signal Processing*, vol. 52, no. 2, pp. 461–471, 2004.

[27] Z. Shen, R. Chen, J. G. Andrews, R. W. Heath, and B. L. Evans, "Low complexity user selection algorithms for multiuser MIMO systems with block diagonalization," *IEEE Transactions on Signal Processing*, vol. 54, no. 9, pp. 3658–3663, 2006.

[28] L. U. Choi and R. D. Murch, "A transmit preprocessing technique for multiuser MIMO systems using a decomposition approach," *IEEE Transactions on Wireless Communications*, vol. 3, no. 1, pp. 20–24, 2004.

[29] K.-K. Wong, "Maximizing the sum-rate and minimizing the sum-power of a broadcast 2-user 2-input multiple-output antenna system using a generalized zeroforcing approach," *IEEE Transactions on Wireless Communications*, vol. 5, no. 12, pp. 3406–3412, 2006.

[30] Z. Pan, K.-K. Wong, and T.-S. Ng, "Generalized multiuser orthogonal space-division multiplexing," *IEEE Transactions on Wireless Communications*, vol. 3, no. 6, pp. 1969–1973, 2004.

[31] P. S. Udupa and J. S. Lehnert, "Optimizing zero-forcing precoders for MIMO broadcast systems," *IEEE Transactions on Communications*, vol. 55, no. 8, pp. 1516–1524, 2007.

[32] A. Wiesel, Y. C. Eldar, and S. Shamai, "Zero-forcing precoding and generalized inverses," *IEEE Transactions on Signal Processing*, vol. 56, no. 9, pp. 4409–4418, 2008.

[33] M. Stojanovic, "Low complexity OFDM detector for underwater acoustic channels," in *IEEE OCEANS*, September 2006, pp. 1–6.

[34] B. Li, S. Zhou, M. Stojanovic, L. Freitag, and P. Willett, "Multicarrier communication over underwater acoustic channels with nonuniform Doppler shifts," *IEEE Journal of Oceanic Engineering*, vol. 33, no. 2, pp. 198–209, 2008.

[35] C. R. Berger, S. Zhou, J. C. Preisig, and P. Willett, "Sparse channel estimation for multicarrier underwater acoustic communication: From subspace methods to compressed sensing," *IEEE Transactions on Signal Processing*, vol. 58, no. 3, pp. 1708–1721, 2010.

[36] Y. V. Zakharov and V. P. Kodanev, "Multipath-Doppler diversity of OFDM signals in an underwater acoustic channel," in *IEEE International Conference on Acoustics, Speech, and Signal Processing*, vol. 5, June 2000, pp. 2941–2944.

[37] S. Roy, T. M. Duman, V. McDonald, and J. G. Proakis, "High-rate communication for underwater acoustic channels using multiple transmitters and space–time coding: Receiver structures and experimental results," *IEEE Journal of Oceanic Engineering*, vol. 32, no. 3, pp. 663–688, 2007.

[38] H. Song, W. Hodgkiss, W. Kuperman, T. Akal, and M. Stevenson, "High-frequency acoustic communications achieving high bandwidth efficiency," *The Journal of the Acoustical Society of America*, vol. 126, no. 2, pp. 561–563, 2009.

[39] Z. Wang, S. Zhou, G. B. Giannakis, C. R. Berger, and J. Huang, "Frequency-domain oversampling for zero-padded OFDM in underwater acoustic communications," *IEEE Journal of Oceanic Engineering*, vol. 37, no. 1, pp. 14–24, 2012.

[40] J. C. Peterson and M. B. Porter, "Ray/beam tracing for modeling the effects of ocean and platform dynamics," *IEEE Journal of Oceanic Engineering*, vol. 38, no. 4, pp. 655–665, 2013.

[41] P. Qarabaqi and M. Stojanovic, "Statistical characterization and computationally efficient modeling of a class of underwater acoustic communication channels," *IEEE Journal of Oceanic Engineering*, vol. 38, no. 4, pp. 701–717, 2013.

[42] M. B. Porter, "The Bellhop manual and users guide: Preliminary draft," *Heat, Light, and Sound Research, Inc., La Jolla, CA, USA, Tech. Rep*, 2011.

[43] C. Liu, Y. V. Zakharov, and T. Chen, "Doubly selective underwater acoustic channel model for a moving transmitter/receiver," *IEEE Transactions on Vehicular Technology*, vol. 61, no. 3, pp. 938–950, 2012.

[44] B. Henson, J. Li, Y. V. Zakharov, and C. Liu, "Waymark baseband underwater acoustic propagation model," in *IEEE Underwater Communications and Networking (UComms)*, Sept 2014, pp. 1–5.

[45] B. Henson, "Waymark based underwater acoustic channel model," Apr. 29 2017, https://www.york.ac.uk/electronic-engineering/research/communication-technologies/underwater-networks/resources/.

[46] L. Liao, B. Henson, and Y. Zakharov, "Grid Waymark baseband underwater acoustic transmission model," in *Underwater Acoustics Conference and Exhibition*, September 2017, pp. 343–350.

[47] S. M. Kay, *Fundamentals of statistical signal processing*. Prentice Hall PTR, 1993.

[48] T. M. Kim, F. Sun, and A. J. Paulraj, "Low-complexity MMSE precoding for coordinated multipoint with per-antenna power constraint," *IEEE Signal Processing Letters*, vol. 20, no. 4, pp. 395–398, 2013.

[49] B. Bandemer, M. Haardt, and S. Visuri, "Linear MMSE multi-user MIMO downlink precoding for users with multiple antennas," in *IEEE International Symposium on Personal, Indoor and Mobile Radio Communications*, December 2006, pp. 1–5.

[50] X. Shao, J. Yuan, and Y. Shao, "Error performance analysis of linear zero forcing and MMSE precoders for MIMO broadcast channels," *IET Communications*, vol. 1, no. 5, pp. 1067–1074, 2007.

[51] N. O. Booth, A. T. Abawi, P. W. Schey, and W. S. Hodgkiss, "Detectability of low-level broad-band signals using adaptive matched-field processing with vertical aperture arrays," *IEEE Journal of Oceanic Engineering*, vol. 25, no. 3, pp. 296–313, 2000.

[52] J. G. Proakis, "Digital communications," *McGraw-Hill*, 1995.
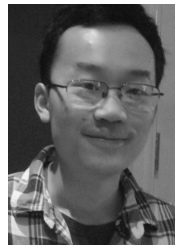
Li Liao received the B.S.degree in Information Engineering from South China University of Technology, Guangzhou, China, in 2012, and the M.Sc. degree with distinction in communications engineering from the University of York, York, U.K., in 2014. Currently, he is pursuing the Ph.D. degree in electronic engineering at the University of York, York, U.K. His current research interests include channel modeling for underwater acoustics and signal processing for communications.

Yuriy V. Zakharov (M'01-SM'08) received the M.Sc. and Ph.D. degrees in electrical engineering from the Power Engineering Institute, Moscow, Russia, in 1977 and 1983, respectively. From 1977 to 1983, he was with the Special Design Agency in the Moscow Power Engineering Institute. From 1983 to 1999, he was with the N. N. Andreev Acoustics Institute, Moscow. From 1994 to 1999, he was with Nortel as a DSP Group Leader. Since 1999, he has been with the University of York, U.K., where he is currently a Reader in the Department of Electronic Engineering. His research interests include signal processing, communications, and acoustics.

Paul Mitchell (M'00-SM'09) received the MEng and PhD degrees from the University of York in 1999 and 2003, respectively. His PhD research was on medium access control for satellite systems, which was supported by British Telecom. He has been a member of the Department of Electronic Engineering at York since 2002, and is currently Senior Lecturer. He has gained industrial experience at BT and QinetiQ. Current research interests include medium access control and networking for underwater and mobile communication systems, and the application of artificial intelligence techniques to such problems. He is currently a lead investigator on EPSRC USMART (EP/P017975/1) and a co-investigator of H2020 MCSA 5G-AURA. Dr Mitchell is an author of over 100 refereed journal and conference papers and he has served on numerous international conference programme committees. He was General Chair of the International Symposium on Wireless Communications Systems which was held in York in 2010, and a Track Chair for IEEE VTC in 2015. He is an Associate Editor of the IET Wireless Sensor Systems journal and the Sage International Journal of Distributed Sensor Networks. Dr Mitchell is a Senior Member of the IEEE, a member of the IET and a Fellow of the Higher Education Academy.